**Lymphatic vessel network injury reduces local tumor control despite preservation of the tumor-draining lymph node**

Lauren N. Liebman, Yang Shen, Zachary S. Buchwald, Zhanna Nepiyushchikh, Zhiming Qi, Andrés J. García, and J. Brandon Dixon

**SUPPLEMENTAL MATERIAL**

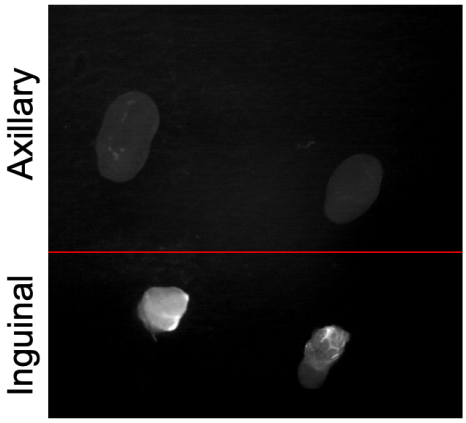


**Supplemental Figure 1. NIR tracer is transported to the inguinal LNs after injection in the flanks.** NIR imaging of axillary (top) and inguinal (bottom) LNs. All 4 LNs were isolated from a single animal sacrificed approximately 10 minutes after subcutaneous injection of tracer in both left and right flanks, then immediately imaged in a single frame.

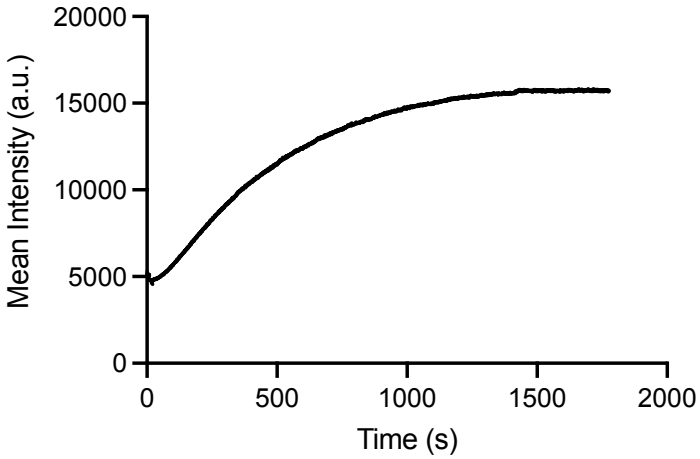


**Supplemental Figure 2. NIR tracer uptake in the LN reaches a plateau within 30 minutes.** Mean intensity of NIR signal in the inguinal LN for 30 minutes (1,800 s) after tracer injection in the flank. Noise during the first minute (60 s) is due to movement artifacts during tracer injection, positioning the animal, and covering the injection site. a.u.: arbitrary units.

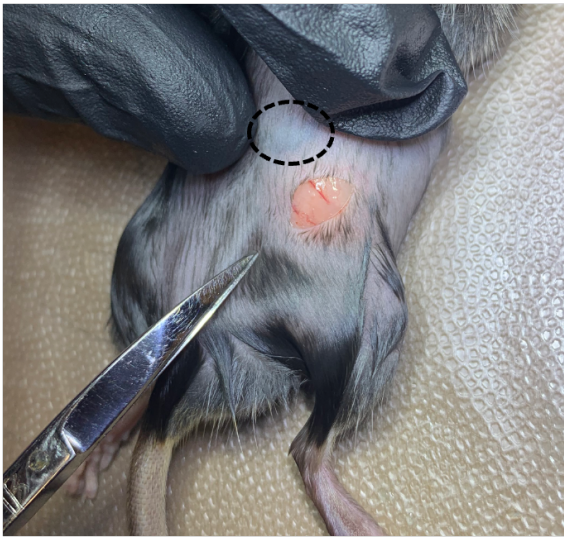

**Supplemental Figure 3. The primary tumor is visible, but not palpable, at time of sham or lymphatic excision surgery.** On Day 3 after primary tumor injection, the tumor could be visualized as a dark, flat mass under the skin (black dashed circle).

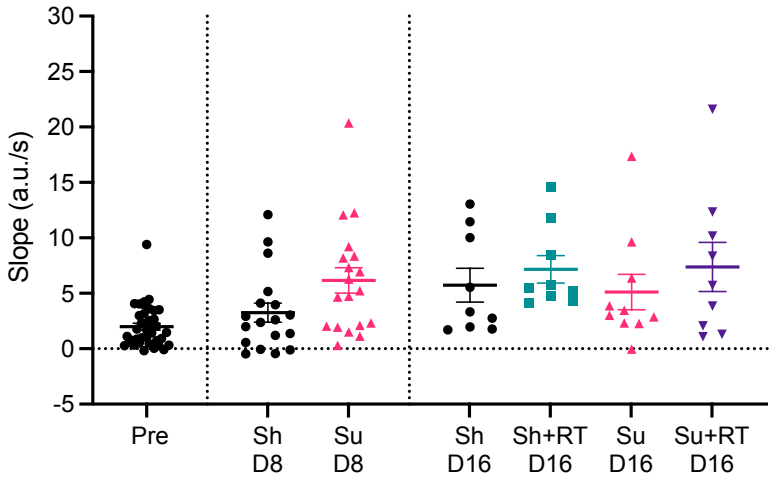


**Supplemental Figure 4. Rate of tracer transport to the tumor-draining lymph node at the distant tumor is not affected by excision of lymphatic tissue.** NIR tracer uptake (slope) for the left TDLN, which drains the contralateral tumor, pre-tumor and on Days 8 and 16. Mixed-effects analysis showed that time had a significant effect ($P<0.0001$) while treatment group did not ($P=0.5795$). Tukey's multiple comparisons test to compare treatment groups at all timepoints found no significant differences between treatment groups. a.u.: arbitrary units; D: day; Pre: pre-tumor; RT: radiotherapy; Sh: sham; Su: lymphatic excision surgery.

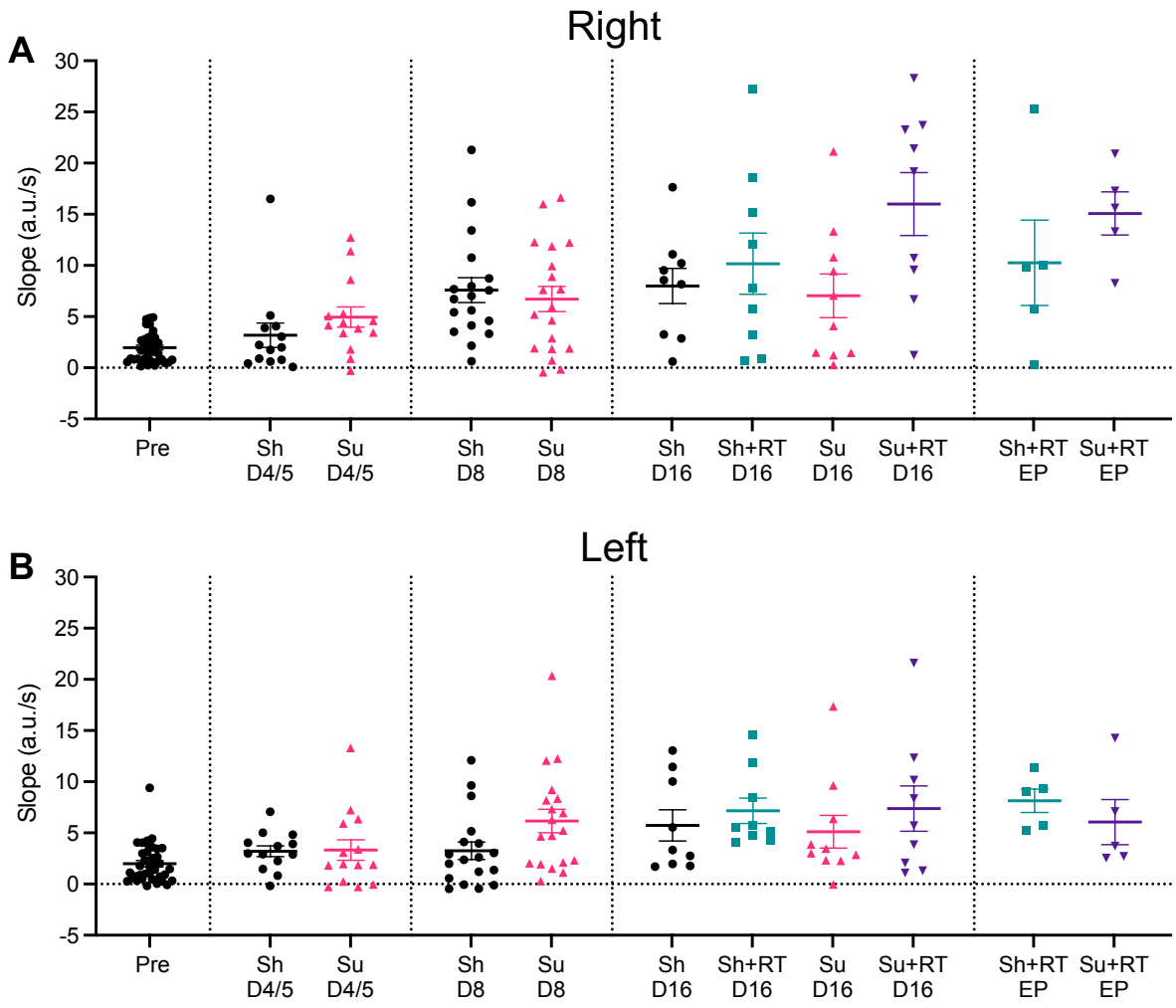


**Supplemental Figure 5: Complete NIR tracer uptake data.** NIR tracer uptake (slope) for **(A)** the right TDLN, which drains the primary tumor, and **(B)** the left TDLN, which drains the contralateral tumor, at all timepoints, including those not used for analysis (Day 4 or 5, endpoint) due to incomplete data. a.u.: arbitrary units; D: day; EP: endpoint; Pre: pre-tumor; RT: radiotherapy; Sh: sham; Su: lymphatic excision surgery.

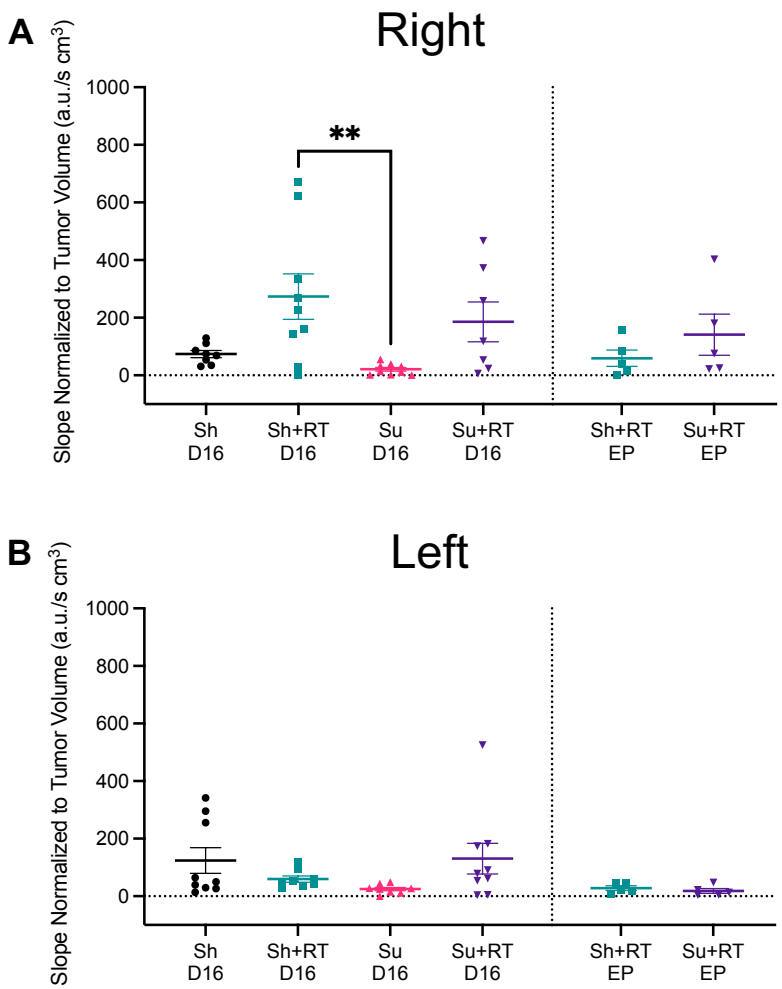


**Supplemental Figure 6: Normalized rate of NIR tracer uptake in the TDLNs.** NIR tracer uptake (slope) normalized to tumor volume in $cm^3$ for **(A)** the right TDLN, which drains the primary tumor, and **(B)** the left TDLN, which drains the contralateral tumor, at Day 16 and endpoint. Ordinary-way ANOVA found significant differences among treatment groups at Day 16 for the primary TDLN (right; P=0.0070), but not for the contralateral TDLN (left; P=0.1585). Tukey's multiple comparisons tests were used for comparisons between all treatment groups at Day 16; all pairwise comparisons were non-significant (P>0.05) unless indicated with asterisks. **P<0.01. a.u.: arbitrary units; D: day; EP: endpoint; Pre: pre-tumor; RT: radiotherapy; Sh: sham; Su: lymphatic excision surgery.

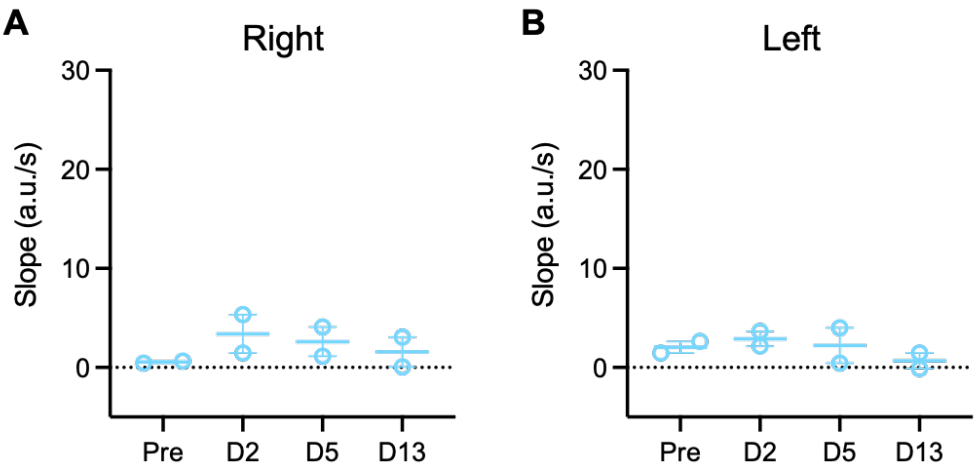


**Supplemental Figure 7. Excision of lymphatic tissue does not disrupt rate of tracer transport to the local or distant LNs in non-tumor bearing mice.** NIR tracer uptake (slope) for the **(A)** right and **(B)** left inguinal LNs before and after lymphatic excision surgery in the right flank on Day 0. No significant effect of time was found by Kruskal-Wallis test for either LN. a.u.: arbitrary units; D: post-surgery day; Pre: pre-surgery.

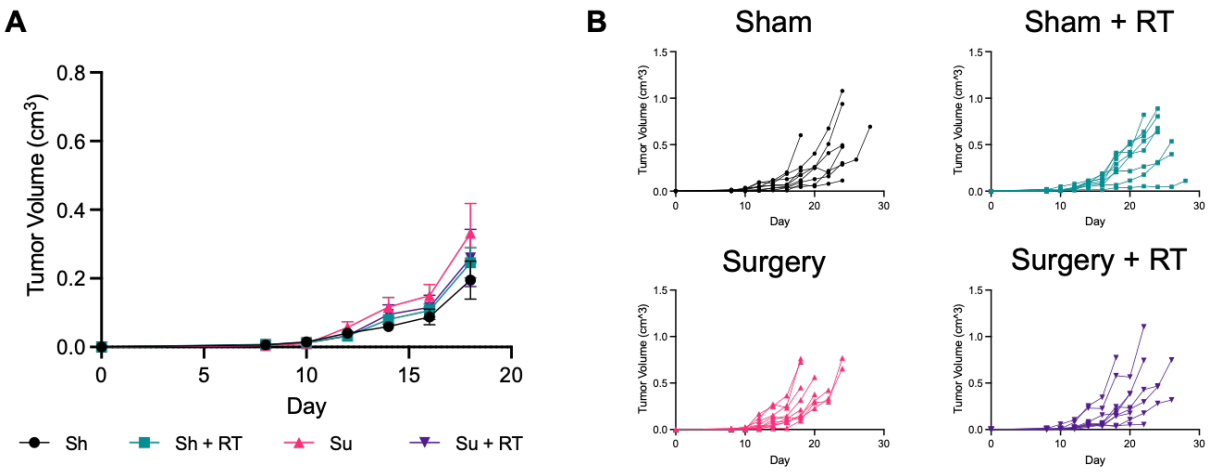


**Supplemental Figure 8. Excision of lymphatic tissue with or without local tumor RT has no effect on distant tumor growth. (A)** Contralateral tumor volumes through Day 18. No significant ($P<0.05$) differences between groups at Day 18 were detected by Tukey's multiple comparisons test. **(B)** Contralateral tumor growth curves for each individual mosue through endpoint.

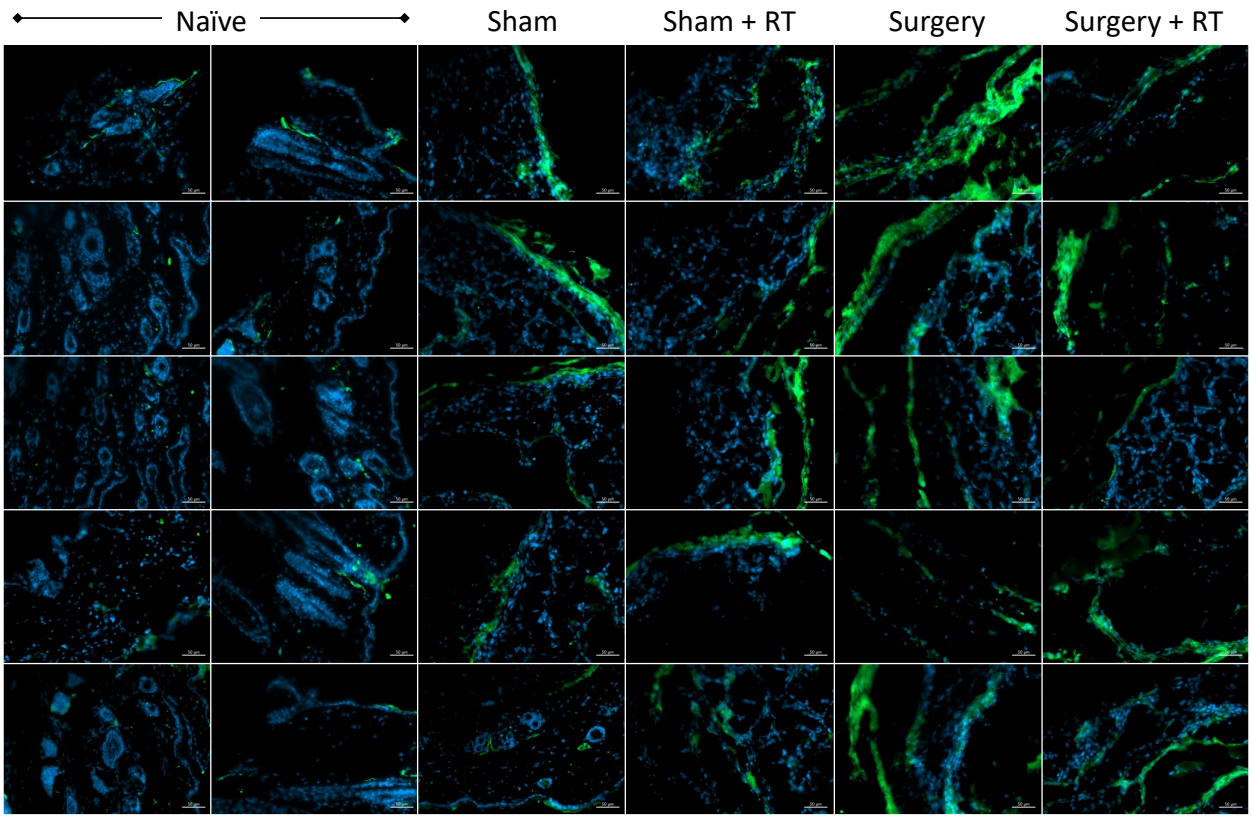


**Supplemental Figure 9. Heterogeneity of podoplanin (PDPN) immunofluorescent staining.** 20x images of naïve skin and tumor periphery. Blue: DAPI. Green: PDPN. All scale bars are 50 μm.

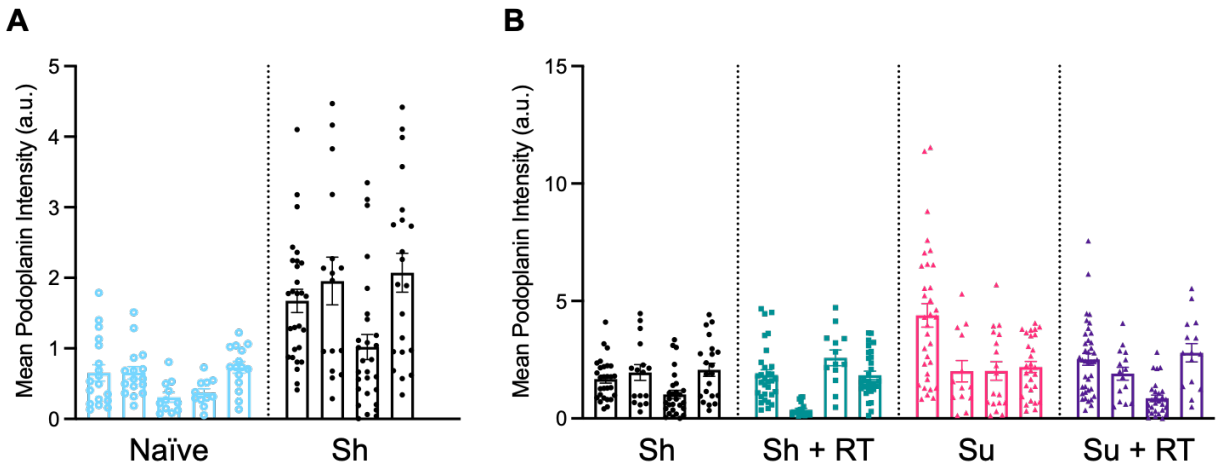


**Supplemental Figure 10. Nested analysis of podoplanin (PDPN) staining intensity.** Each point represents a single image, and each bar represents an animal. Outliers were removed by ROUT. **(A)** Mean PDPN staining intensity for naïve (non-tumor bearing) and sham animals. Number of analyzed images per mouse from left to right: Naïve: 18, 16, 11, 11, 15; Sh: 28, 16, 28, 21. **(B)** Mean PDPN staining intensity for treatment groups. Number of analyzed images per mouse from left to right: Sh: 28, 16, 28, 21; Sh + RT: 31, 20, 13, 30; Su: 33, 13, 18, 28; Su + RT: 39, 15, 28, 15. a.u.: arbitrary units; RT: radiotherapy; Sh: sham; Su: lymphatic excision surgery.

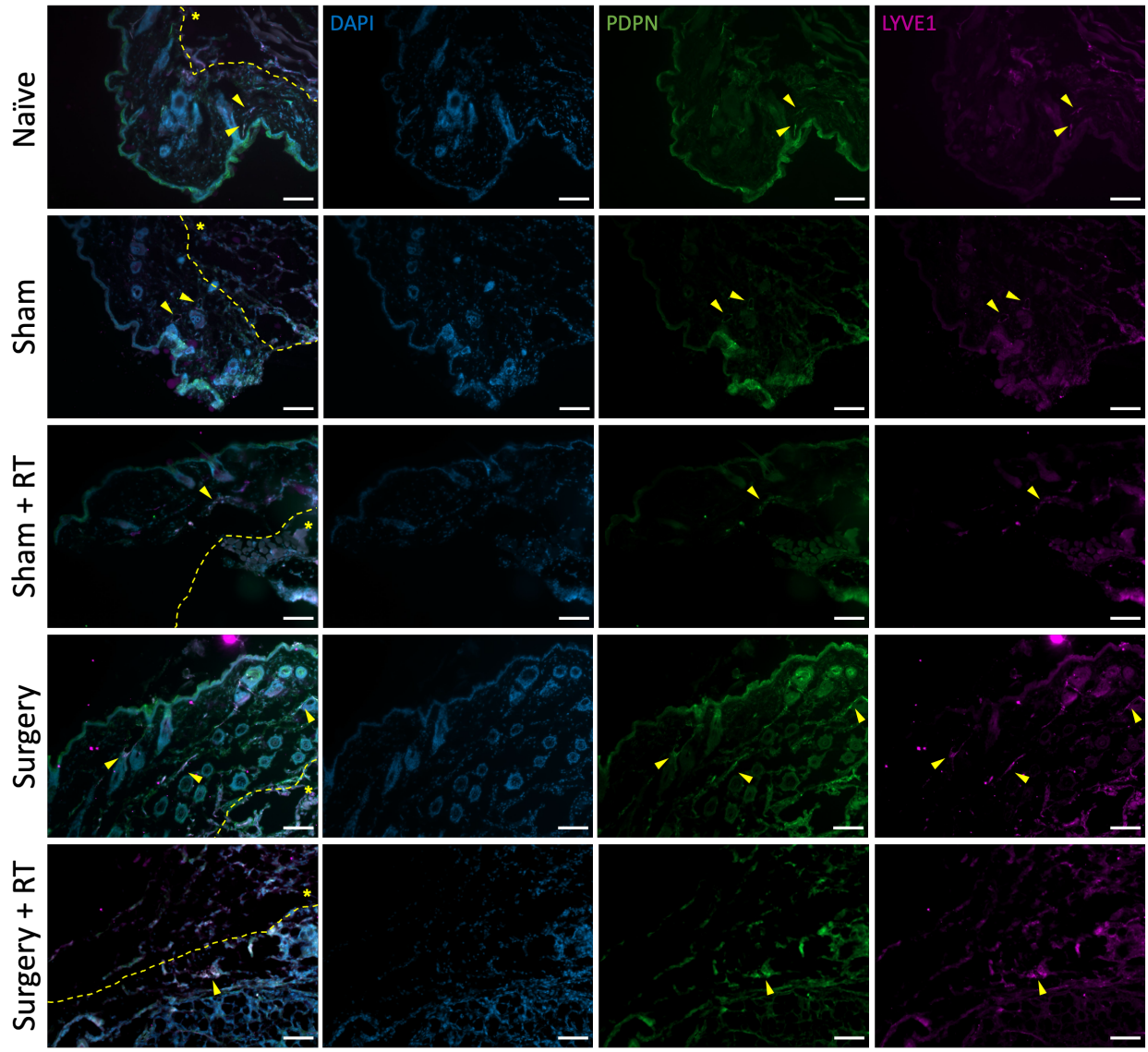


**Supplemental Figure 11. Lymphatic vessel endothelial hyaluronan receptor 1 (LYVE1) staining.** Representative composite and single-channel 10x images of naïve skin and tumor periphery. Blue: DAPI. Green: PDPN. Magenta: LYVE1. All scale bars are 100 μm. Tumor borders are in composite images by dotted yellow lines, with yellow asterisks indicating which side is the tumor stroma. Yellow arrowheads in composite, single-channel PDPN, and single-channel LYVE1 images indicate double-positive (PDPN and LYVE1) lymphatic vessels.

**Supplemental Table 1. Pearson correlation coefficient (PCC) for LYVE1 and PDPN colocalization in stained sections.** PCC is reported ± SEM. 10 images were analyzed per group.

| Group | PCC |
|---|---|
| Naïve | 0.8823 ± 0.0139 |
| Sham | 0.8057 ± 0.0180 |
| Sham + RT | 0.9564 ± 0.0073 |
| Surgery | 0.9724 ± 0.0082 |
| Surgery + RT | 0.8615 ± 0.0379 |

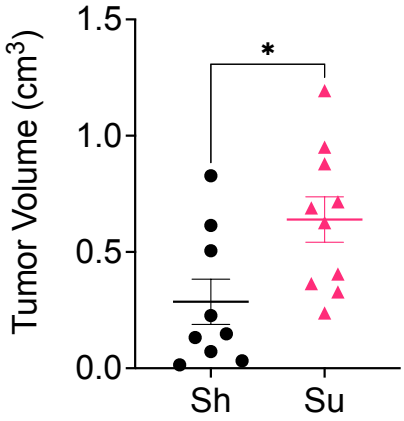


**Supplemental Figure 12. Lymphatic excision surgery increases tumor volume at Day 17 in a unilateral melanoma model.** Sham N=9; Lymphatic excision surgery N=10. Asterisk indicates P value from unpaired t test. *P<0.05. Sh: sham; Su: lymphatic excision surgery.

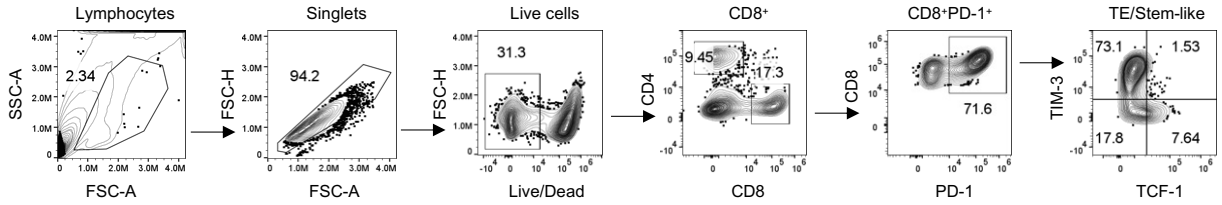


**Supplemental Figure 13. Flow cytometry gating strategy.** Representative flow cytometry plots demonstrating the gating strategy applied for this study. FSC-A: forward scatter area; FSC-H: forward scatter height; SSC-A: side scatter area; TE: terminally differentiated effector-like.

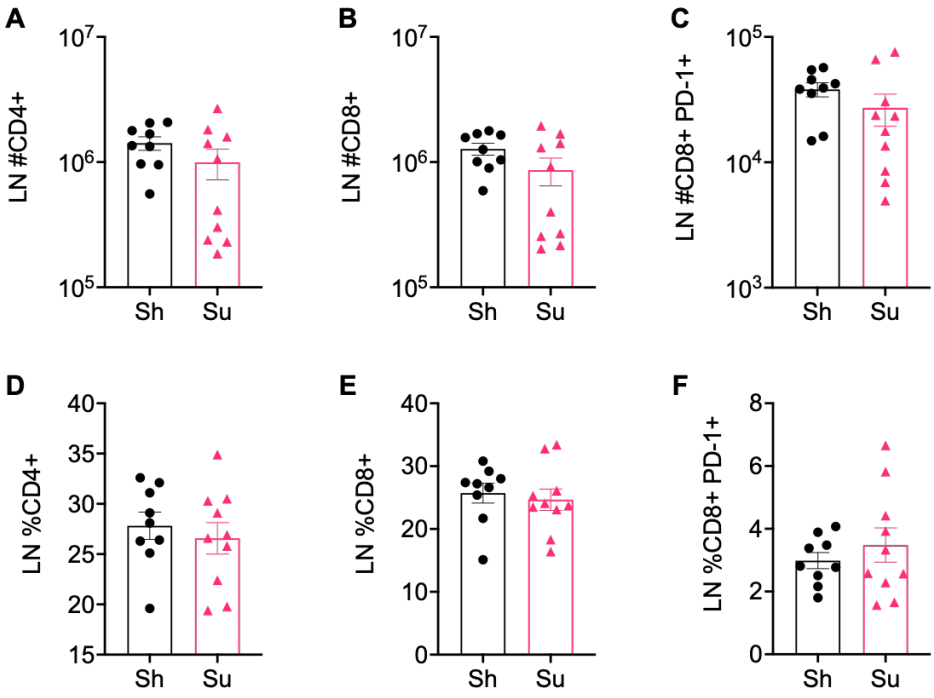


**Supplemental Figure 14. Lymphatic excision surgery does not alter T cell populations in the LN.** Numbers of **(A)** $CD4^+$, **(B)** $CD8^+$, and **(C)** $CD8^+$ $PD\text{-}1^+$ lymphocytes in the TDLN. Percentages of **(D)** $CD4^+$, **(E)** $CD8^+$, and **(F)** $CD8^+$ $PD\text{-}1^+$ lymphocytes in the TDLN. Sham N=9; Lymphatic excision surgery N=10. No significant differences ($P<0.05$) were detected by unpaired t tests. Sh: sham; Su: lymphatic excision surgery.

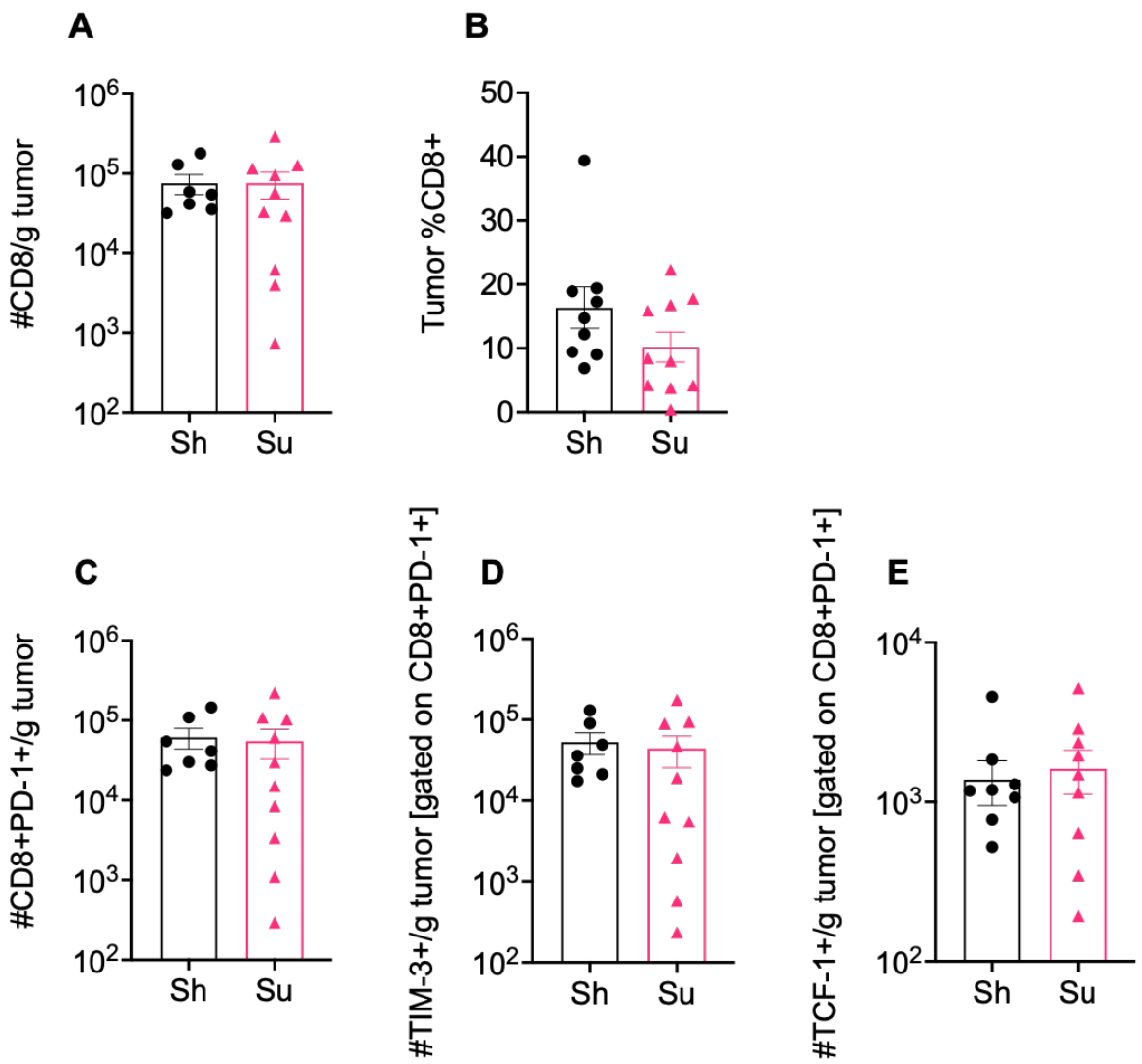


**Supplemental Figure 15. Lymphatic excision surgery reduces percentage, but not number, of CD8$^+$ PD-1$^+$ and Tim-3$^+$ T cells in the tumor. (A)** Numbers and **(B)** percentages CD8$^+$ lymphocytes in the tumor, normalized by tumor weight. Numbers of **(C)** CD8$^+$ PD-1$^+$, **(D)** Tim-3$^+$ (CD8$^+$ PD-1$^+$), and **(E)** TCF-1$^+$ (CD8$^+$ PD-1$^+$) lymphocytes in the tumor, normalized by tumor weight. Sham N=9; Lymphatic excision surgery N=10. No significant ($P<0.05$) differences were detected by unpaired t tests. Sh: sham; Su: lymphatic excision surgery.

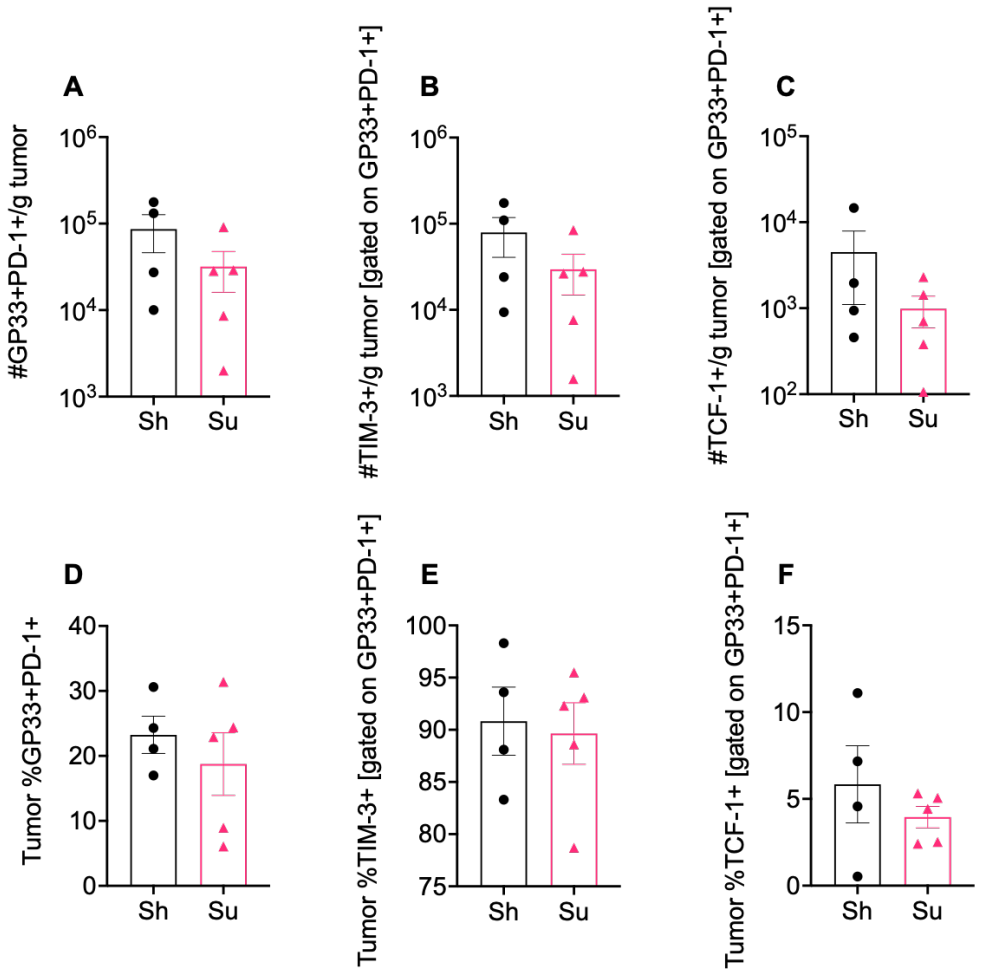


**Supplemental Figure 16. Lymphatic excision surgery may not alter tumor-specific (GP33$^+$) T cell populations in the tumor.** Numbers of **(A)** GP33$^+$ PD-1$^+$, **(B)** Tim-3$^+$ GP33$^+$ PD-1$^+$, **(C)** and TCF-1$^+$ GP33$^+$ PD-1$^+$ lymphocytes in the tumor, normalized by tumor weight. Percentages of **(D)** GP33$^+$ PD-1$^+$, **(E)** Tim-3$^+$ GP33$^+$ PD-1$^+$, **(F)** and TCF-1$^+$ GP33$^+$ PD-1$^+$ lymphocytes in the tumor. Sham N=4; Lymphatic excision surgery N=5. No significant ($P<0.05$) differences were detected by unpaired t tests. Sh: sham; Su: lymphatic excision surgery.